Acta Cryst E
CRYSTALLOGRAPHIC COMMUNICATIONS

ISSN 2056-9890

Synthesis and structure of ammonium bis(malonato)borate

Gokila Govindharajan,[a] Ramachandra Raja Chidambaram,[b] Gnanasheela Uthamaselvan,[c] Kalaiarasi Iyathurai,[c] Kamatchi Karthikeyan[d] and Sampath Natarajan[e]*

[a]Government College for Women (Affiliated to Bharathidasan University), Kumbakonam,Thanjavur, Tamilnadu-612001, India, [b]Department of Physics, D. G. Government Arts College for Women (Affiliated to Annamalai University), Mayiladuthurai, Taminadu-609 001, India, [c]Department of Physics, Government College for Women (Affiliated to Bharathidasan University), Kumbakonam, Thanjavur, Tamilnadu-612001, India, [d]Department of Physics, Srinivasa Ramanujan Centre, SASTRA Deemed University, Kumbakonam, Thanjavur, Tamilnadu-612001, India, and [e]Department of Chemistry, Chemical Biology Lab., School of Chemical and Biotechnology, SASTRA Deemed University, Thanjavur, Tamilnadu-613401, India. *Correspondence e-mail: sampath@scbt.sastra.edu

Received 16 July 2025
Accepted 9 August 2025

Edited by W. T. A. Harrison, University of Aberdeen, United Kingdom

Keywords: crystal structure; ammonium; bis(malonato)borate; Hirshfeld surface.

CCDC reference: 2455003

Supporting information: this article has supporting information at journals.iucr.org/e

In the title salt, $NH_4^+\cdot[B(C_3H_2O_4)_2]^-$, the boron atom is chelated by two malonate ligands in a bidentate fashion, resulting in a BO_4 tetrahedron with both chelate rings adopting shallow boat conformations. The extended structure features five N—H···O and three C—H···O hydrogen bonds, accounting for approximately 69.9% of the total intermolecular interactions.

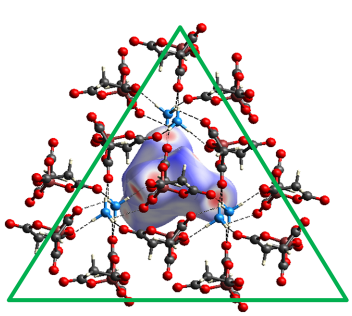

1. Chemical context

The bis(malonate)borate anion, $[B(C_3H_2O_4)_2]^-$, is a tetrahedral boron-centred complex in which two malonate ligands are bidentately coordinated *via* their carboxylate oxygen atoms. This chelation results in a stable, symmetrical anion capable of forming extended hydrogen-bonded or ionic frameworks when paired with alkali metal cations such as sodium or potassium (Zviedre & Belyakov, 2007; Selvi *et al.*, 2024). In materials science, bis(malonate)borate derivatives have attracted attention for their role in energy storage technologies. The lithium and sodium salts of this anion have been explored as polymeric ion conductors and electrolyte additives in lithium ion and sodium ion batteries, where their borate anions contribute to enhanced electrochemical stability and ionic conductivity (Mahanthappa & Weber, 2015).

In tribological applications, bis(malonate)borate-based ionic liquids have shown excellent thermal stability and anti-wear performance, making them environmentally friendly alternatives to halogenated lubricants (Gusain & Khatri, 2015). In biological contexts, although less studied, the malonate ligands mimic natural chelators, suggesting potential applications in metal detoxification and enzyme inhibition. Furthermore, the aqueous solubility and biocompatibility of boron-containing compounds, including bis(malonate)borates, position them as potential boron delivery agents in boron neutron capture therapy (BNCT) for cancer treatment (Järvinen *et al.*, 2023; Li *et al.*, 2025; Dymova *et al.*, 2020). These multifaceted properties underscore the growing interest in bis(malonate)borate anions at the intersection of green chemistry, energy materials and biomedical innovation. As part of our work in this area, we now describe the synthesis and structure of the title compound, $NH_4^+[B(C_3H_2O_4)_2]^-$, (**I**).

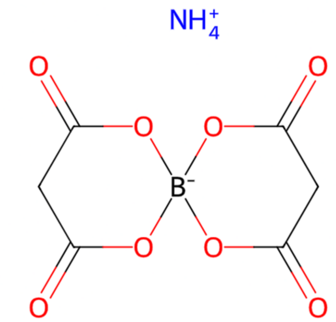

2. Structural commentary

Compound (**I**) features a presumed sp^3-hybridized tetrahedral B atom coordinated by two chelating malonate ligands, each binding through two carboxylate O atoms (Fig. 1). Selected geometrical data are given in Table 1. In the B—O tetrahedron, the mean B—O bond length of 1.465 Å is in good agreement with the already reported structure of sodium bis(malonate)borate (Selvi *et al.* 2024) and also agrees with the expected value for a Bsp^3—O bond length (1.468 Å; Allen *et al.*, 1987). The largest O—B—O bond angles are the intracyclic angles: O1—B1—O3 = 112.4 (2)° and O5—B1—O6 = 112.5 (2)°. The six-membered boro–malonate rings B1/O5/C4/C5/C6/O6 (Fig. 2*a*) and B1/O1/C1/C2/C3/O3 (Fig. 2*b*) both adopt shallow boat conformations with puckering amplitudes Q_T = 0.457 (2) and 0.414 (2) Å, respectively. In the boat conformations of the boro-malonate rings (Fig. 2), atoms B1 and C2 deviate from the near planarity of other atoms (O3, C3, C1, and O1) by −0.413 (2) and −0.378 (2) Å, respectively. In the other ring, atoms B1 and C5 deviate from the mean plane of the other atoms (O5, C4, C6 and O6) by 0.386 (2) and 0.330 (2) Å, respectively. The dihedral angle between the boro-malonate rings is 76.5 (1)°, *i.e.*, they are oriented almost perpendicular to each other. The $[B(C_3H_2O_4)_2]^-$ anion is charge balanced by NH_4^+ cations, which participate in an extensive hydrogen-bonded network.

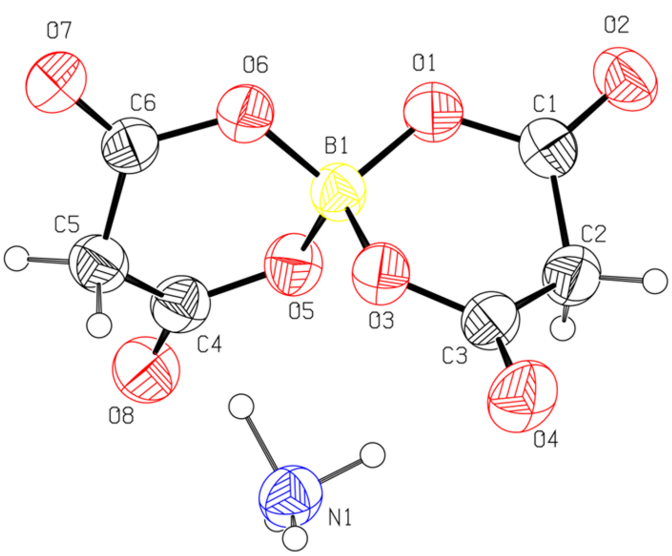

Figure 1
The molecular structure of (**I**) showing 50% displacement ellipsoids.

Table 1
Selected geometric parameters (Å, °).

B1—O1	1.457 (3)	B1—O5	1.474 (3)
B1—O3	1.472 (3)	B1—O6	1.454 (3)
O1—B1—O3	112.42 (17)	O6—B1—O1	105.67 (17)
O1—B1—O5	108.36 (18)	O6—B1—O3	108.43 (18)
O3—B1—O5	109.46 (18)	O6—B1—O5	112.51 (17)

Table 2
Hydrogen-bond geometry (Å, °).

D—H···*A*	*D*—H	H···*A*	*D*···*A*	*D*—H···*A*
N1—H1*A*···O2^{i}	0.88 (2)	2.41 (2)	3.103 (3)	137 (2)
N1—H1*A*···O4^{ii}	0.88 (2)	2.43 (2)	3.166 (3)	142 (2)
N1—H1*B*···O4^{iii}	0.83 (2)	2.32 (2)	2.970 (3)	136 (3)
N1—H1*C*···O7	0.86 (2)	2.03 (2)	2.864 (3)	165 (3)
N1—H1*D*···O8^{iv}	0.87 (2)	2.13 (2)	2.985 (3)	168 (3)
C2—H2*A*···O7^{v}	0.97	2.33	3.218 (3)	153
C2—H2*B*···O2^{vi}	0.97	2.48	3.181 (3)	129
C5—H5*B*···O6^{vii}	0.97	2.48	3.289 (3)	140

Symmetry codes: (i) $-x+1, -y+2, -z+1$; (ii) $-x+1, y+\frac{1}{2}, -z+\frac{1}{2}$; (iii) $x+1, -y+\frac{3}{2}, z+\frac{1}{2}$; (iv) $x, y+1, z$; (v) $x-1, y, z$; (vi) $-x, -y+1, -z+1$; (vii) $-x+1, y-\frac{1}{2}, -z+\frac{1}{2}$.

3. Supramolecular features

The structural integrity of the extended structure of (**I**) is maintained by a network of N—H···O and C—H···O interactions (Fig. 3), as detailed in Table 2. Each $[B(C_3H_2O_4)_2]^-$ anion accepts hydrogen bonds from five neighbouring NH_4^+

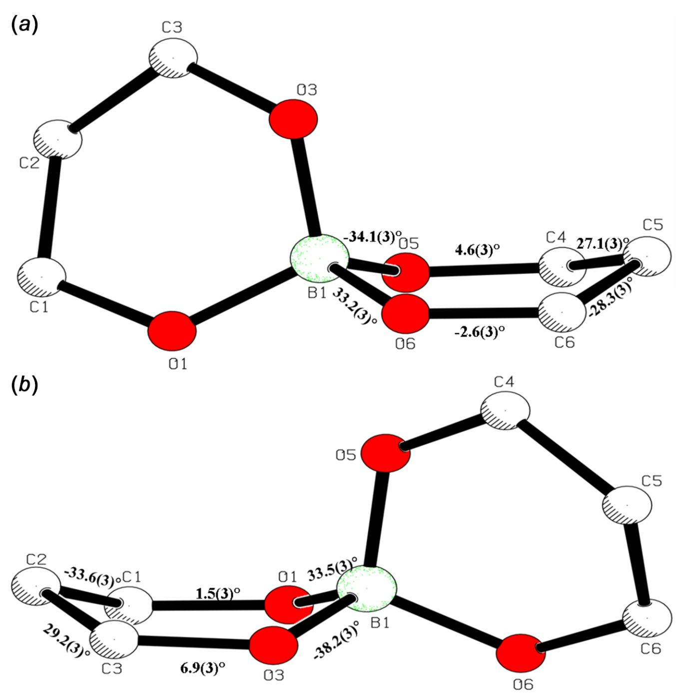

Figure 2
Side views of the chelate rings in (**I**) with torsion angles indicated.

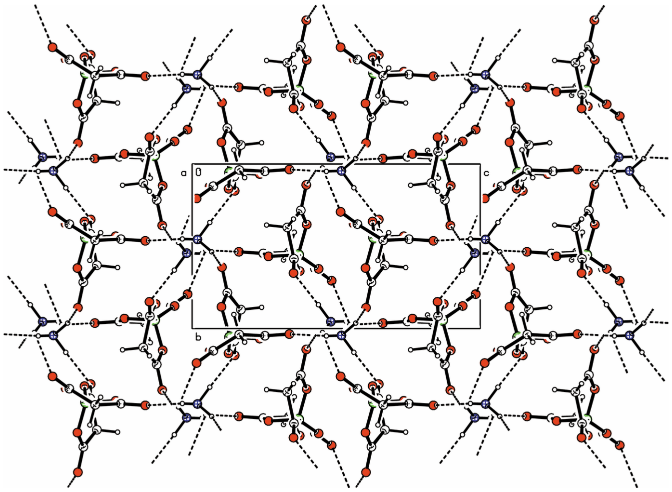

Figure 3
Packing diagram for (**I**) viewed down the *a*-axis direction. The dotted lines indicate the hydrogen bonds.

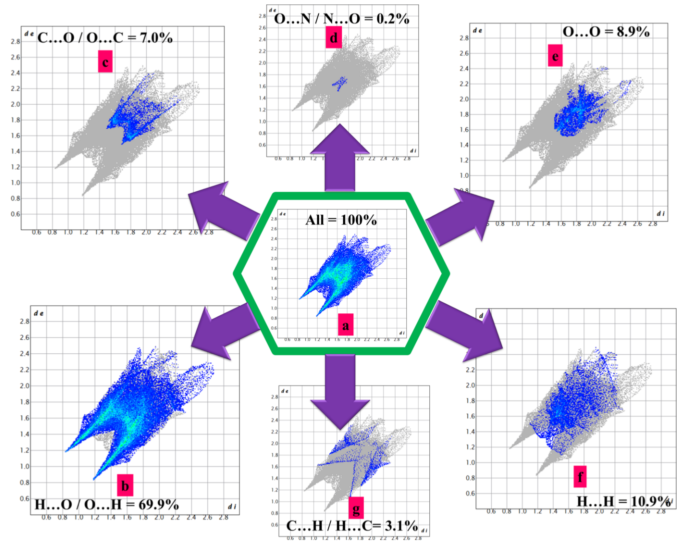

Figure 5
Fingerprint plots for (**I**).

cations (Fig. 4*a*). Conversely, every NH_4^+ cation participates in analogous interactions with five adjacent $[B(C_3H_2O_4)_2]^-$ anions (Fig. 4*b*). This results in the formation of a triangular-shaped supramolecular assembly (Fig. 4*c*).

Hirshfeld surface analysis of (**I**) was performed using *Crystal Explorer* (Version 21.5; Spackman *et al.*, 2021). Fig. 4*d* shows the d_{norm} surface for the $[B(C_3H_2O_4)_2]^-$ anion where the intense red spots signify the shortest contacts (indicative of strong hydrogen bonds) and blue regions denote longer distances (suggesting weak van der Waals or repulsive interactions). Fig. 5 shows the two-dimensional fingerprint plots, with the overall interaction in Fig. 5*a* and the decomposed contributions and their percentages in Fig. 5*b*–5*g*. The hydrogen bonds are distinctly marked by sharp, symmetrical wings in the H···O/O···H plot (Fig. 5*b*), which dominates the Hirshfeld surface (69.9%).

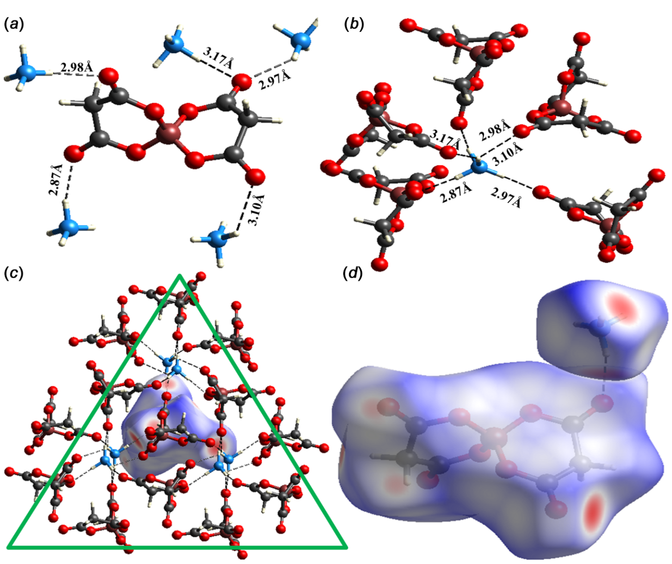

Figure 4
The environments of (*a*) the cation, (*b*) the anion and (*c*) the triangular supramolecular motif in (**I**); (*d*) the Hirshfeld surface for (**I**).

4. Database survey

A search of the Cambridge Structural Database (CSD 2025; Groom *et al.*, 2016) using CCDC CONQUEST revealed two related bis(malonate)borate complexes, CSD refcode PODHAV (Selvi *et al.*, 2024) and PITQUF (Zviedre & Belyakov, 2007), featuring Na^+ and K^+ counter-ions, respectively. While these exhibit malanato-borate coordination geometries very similar to (**I**), they differ fundamentally through their alkali metal coordination spheres as opposed to our ammonium variant. Notably, the potassium centre in PITQUF adopts an irregular nine-coordinate geometry with oxygen donors from seven distinct anions, whereas the sodium centre in PODHAV displays an intermediate coordination state – primarily square pyramidal (five O-donors) but transitioning to a distorted octahedron upon inclusion of a sixth, more weakly bound oxygen atom.

5. Synthesis and crystallization

A mixture of malonic acid, boric acid, and ammonium carbonate in a molar ratio of 4:2:1 was dissolved in double-distilled water while continuously stirring. The solution was gently heated to a temperature of 313–323 K to ensure complete dissolution, resulting in a clear, homogeneous mixture. It was then allowed to cool to room temperature and was filtered to remove any particulate impurities. The filtrate was transferred to a clean glass vessel, which was covered with a perforated lid to control evaporation, and placed in a draft-free environment maintained at a temperature of 298–303 K. Over a period of 60 days, slow evaporation of the solvent led to the growth of well-defined colourless blocks of (**I**). These were carefully extracted, rinsed with cold distilled water to eliminate surface impurities, and air-dried at room temperature.

6. Refinement

Crystal data, data collection and structure refinement details are summarised in Table 3. The carbon-bound hydrogen atoms were positioned based on calculated values (C—H = 0.96 Å) and were refined as riding atoms, with U_{iso}(H) set to 1.2 U_{eq}(C). For the NH_4^+ ion, the hydrogen atoms were refined using DFIX restraints, maintaining an N—H distance of 0.86 Å and setting U_{iso}(H) to 1.4U_{eq}(N).

Acknowledgements

The authors thank the Sophisticated Analytical Instrument Facility (SAIF), Indian Institute of Technology Madras (IITM), Chennai, Tamilnadu, India, for the single-crystal X-ray diffraction data. GG, UG and IK gratefully acknowledge the infrastructural facilities at the DST–CURIE lab (DST-CURIE–PG/2022/54).

Table 3
Experimental details.

Crystal data	
Chemical formula	$NH_4^+ \cdot C_6H_4BO_8^-$
M_r	232.94
Crystal system, space group	Monoclinic, $P2_1/c$
Temperature (K)	298
a, *b*, *c* (Å)	9.1825 (7), 7.6234 (6), 13.6905 (10)
β (°)	102.201 (2)
V (Å^3)	936.71 (12)
Z	4
Radiation type	Cu *Kα*
μ (mm^{-1})	1.36
Crystal size (mm)	0.23 × 0.16 × 0.13
Data collection	
Diffractometer	Bruker D8 VENTURE
Absorption correction	Multi-scan (*SADABS*; Krause *et al.*, 2015)
T_{min}, T_{max}	0.526, 0.753
No. of measured, independent and observed [$I > 2\sigma(I)$] reflections	14514, 1771, 1631
R_{int}	0.060
$(\sin \theta/\lambda)_{max}$ (Å^{-1})	0.610
Refinement	
$R[F^2 > 2\sigma(F^2)]$, $wR(F^2)$, *S*	0.066, 0.211, 1.15
No. of reflections	1771
No. of parameters	158
No. of restraints	10
H-atom treatment	H atoms treated by a mixture of independent and constrained refinement
$\Delta\rho_{max}$, $\Delta\rho_{min}$ (e Å^{-3})	0.22, −0.27

Computer programs: *APEX4* and *SAINT* (Bruker, 2021), *SHELXT2018/2* (Sheldrick, 2015*a*), *SHELXL2019/3* (Sheldrick, 2015*b*) and *OLEX2* (Dolomanov *et al.*, 2009).

References

Allen, F. H., Kennard, O., Watson, D. G., Brammer, L., Orpen, A. G. & Taylor, R. (1987). *J. Chem. Soc. Perkin Trans. 2* pp. S1–19.

Bruker (2021). *APEX3, SAINT* and *XPREP*. Bruker AXS Inc., Madison, Wisconsin, USA.

Dolomanov, O. V., Bourhis, L. J., Gildea, R. J., Howard, J. A. K. & Puschmann, H. (2009). *J. Appl. Cryst.* **42**, 339–341.

Dymova, M. A., Taskaev, S. Y., Richter, V. A. & Kuligina, E. V. (2020). *Cancer Commun.* **40**, 406–421.

Groom, C. R., Bruno, I. J., Lightfoot, M. P. & Ward, S. C. (2016). *Acta Cryst.* B**72**, 171–179.

Gusain, R. & Khatri, O. P. (2015). *RSC Adv.* **5**, 25399–25408.

Järvinen, J., Pulkkinen, H., Rautio, J. & Timonen, J. M. (2023). *Pharmaceutics* **15**, 2663.

Krause, L., Herbst-Irmer, R., Sheldrick, G. M. & Stalke, D. (2015). *J. Appl. Cryst.* **48**, 3–10.

Li, X., He, P., Wei, Y., Qu, C., Tang, F. & Li, Y. (2025). *Cancer Nano* **16**, 25.

Mahanthappa, M. K. & Weber, R. L. (2015). US Patent US9221844B2.

Selvi, R., Gokila, G., Thiruvalluvar, A. A. & Sundararajan, R. S. (2024). *Acta Cryst.* E**80**, 180–183.

Sheldrick, G. M. (2015*a*). *Acta Cryst.* A**71**, 3–8.

Sheldrick, G. M. (2015*b*). *Acta Cryst.* C**71**, 3–8.

Spackman, P. R., Turner, M. J., McKinnon, J. J., Wolff, S. K., Grimwood, D. J., Jayatilaka, D. & Spackman, M. A. (2021). *J. Appl. Cryst.* **54**, 1006–1011.

Zviedre, I. I. & Belyakov, S. V. (2007). *Russ. J. Inorg. Chem.* **52**, 686–690.

supporting information

Acta Cryst. (2025). E**81**, 849-852 [https://doi.org/10.1107/S2056989025007169]

Synthesis and structure of ammonium bis(malonato)borate

Gokila Govindharajan, Ramachandra Raja Chidambaram, Gnanasheela Uthamaselvan, Kalaiarasi Iyathurai, Kamatchi Karthikeyan and Sampath Natarajan

Computing details

Ammonium bis(malonato)borate

Crystal data

$NH_4^+ \cdot C_6H_4BO_8^-$
M_r = 232.94
Monoclinic, $P2_1/c$
a = 9.1825 (7) Å
b = 7.6234 (6) Å
c = 13.6905 (10) Å
β = 102.201 (2)°
V = 936.71 (12) Å^3
Z = 4
F(000) = 480
D_x = 1.652 Mg m^{-3}
Cu $K\alpha$ radiation, λ = 1.54178 Å
Cell parameters from 9961 reflections
θ = 4.9–70.2°
μ = 1.36 mm^{-1}
T = 298 K
Block, colourless
0.23 × 0.16 × 0.13 mm

Data collection

Bruker D8 VENTURE diffractometer
ω and phi scans
Absorption correction: multi-scan (SADABS; Krause *et al.*, 2015)
T_{min} = 0.526, T_{max} = 0.753
14514 measured reflections
1771 independent reflections
1631 reflections with $I > 2\sigma(I)$
R_{int} = 0.060
θ_{max} = 70.2°, θ_{min} = 4.9°
h = −11→10
k = −9→9
l = −16→16

Refinement

Refinement on F^2
Least-squares matrix: full
$R[F^2 > 2\sigma(F^2)]$ = 0.066
$wR(F^2)$ = 0.211
S = 1.15
1771 reflections
158 parameters
10 restraints
Primary atom site location: dual
Hydrogen site location: mixed
H atoms treated by a mixture of independent and constrained refinement
$w = 1/[\sigma^2(F_o^2) + (0.1464P)^2 + 0.136P]$ where $P = (F_o^2 + 2F_c^2)/3$
$(\Delta/\sigma)_{max}$ < 0.001
$\Delta\rho_{max}$ = 0.22 e Å^{-3}
$\Delta\rho_{min}$ = −0.27 e Å^{-3}
Extinction correction: *SHELXL2019/3* (Sheldrick, 2015b), $Fc^*=kFc[1+0.001xFc^2\lambda^3/\sin(2\theta)]^{-1/4}$
Extinction coefficient: 0.027 (5)

Special details

Geometry. All esds (except the esd in the dihedral angle between two l.s. planes) are estimated using the full covariance matrix. The cell esds are taken into account individually in the estimation of esds in distances, angles and torsion angles; correlations between esds in cell parameters are only used when they are defined by crystal symmetry. An approximate (isotropic) treatment of cell esds is used for estimating esds involving l.s. planes.

Fractional atomic coordinates and isotropic or equivalent isotropic displacement parameters (Å²)

	x	*y*	*z*	U_{iso}*/U_{eq}
B1	0.3161 (3)	0.5528 (3)	0.36828 (18)	0.0533 (6)
C1	0.0934 (2)	0.6346 (3)	0.42603 (16)	0.0555 (6)
C2	0.0119 (3)	0.5359 (3)	0.33643 (18)	0.0613 (6)
H2A	−0.088477	0.582327	0.317487	0.074*
H2B	0.004154	0.414022	0.354991	0.074*
C3	0.0825 (2)	0.5434 (3)	0.24711 (16)	0.0558 (6)
C4	0.4578 (2)	0.2814 (3)	0.37743 (15)	0.0557 (6)
C5	0.5646 (3)	0.3847 (3)	0.33053 (17)	0.0577 (6)
H5A	0.663211	0.334372	0.352036	0.069*
H5B	0.536011	0.370650	0.258602	0.069*
C6	0.5738 (2)	0.5760 (3)	0.35371 (15)	0.0540 (6)
O1	0.24075 (17)	0.6373 (2)	0.43926 (11)	0.0607 (5)
O2	0.0333 (2)	0.7096 (2)	0.48443 (13)	0.0699 (6)
O3	0.22873 (16)	0.5613 (2)	0.26507 (10)	0.0567 (5)
O4	0.0112 (2)	0.5335 (3)	0.16249 (13)	0.0808 (7)
O5	0.34322 (16)	0.3679 (2)	0.39802 (11)	0.0580 (5)
O6	0.45349 (16)	0.6506 (2)	0.37350 (12)	0.0587 (5)
O7	0.68341 (18)	0.6631 (2)	0.35204 (15)	0.0691 (6)
O8	0.47475 (19)	0.1267 (2)	0.39622 (13)	0.0702 (6)
N1	0.7675 (2)	0.9580 (2)	0.48129 (16)	0.0622 (6)
H1A	0.833 (3)	1.024 (3)	0.461 (2)	0.093*
H1B	0.792 (3)	0.944 (4)	0.5427 (12)	0.093*
H1C	0.759 (3)	0.863 (3)	0.4469 (19)	0.093*
H1D	0.683 (2)	1.013 (3)	0.465 (2)	0.093*

Atomic displacement parameters (Å²)

	U^{11}	U^{22}	U^{33}	U^{12}	U^{13}	U^{23}
B1	0.0510 (12)	0.0578 (13)	0.0505 (12)	0.0042 (9)	0.0090 (9)	−0.0001 (9)
C1	0.0598 (12)	0.0537 (11)	0.0550 (12)	0.0032 (8)	0.0166 (9)	0.0023 (8)
C2	0.0538 (12)	0.0726 (14)	0.0583 (13)	−0.0037 (9)	0.0138 (10)	−0.0060 (9)
C3	0.0547 (11)	0.0614 (13)	0.0482 (11)	0.0031 (8)	0.0042 (9)	−0.0001 (8)
C4	0.0569 (12)	0.0572 (12)	0.0500 (11)	0.0025 (8)	0.0046 (8)	0.0003 (8)
C5	0.0611 (12)	0.0578 (12)	0.0553 (12)	0.0022 (9)	0.0145 (9)	−0.0041 (9)
C6	0.0519 (11)	0.0608 (12)	0.0470 (10)	0.0009 (9)	0.0053 (8)	−0.0031 (8)
O1	0.0577 (9)	0.0739 (11)	0.0494 (9)	0.0029 (7)	0.0088 (7)	−0.0083 (6)
O2	0.0768 (11)	0.0700 (11)	0.0693 (11)	0.0040 (8)	0.0301 (9)	−0.0108 (7)
O3	0.0542 (9)	0.0702 (10)	0.0463 (9)	0.0030 (6)	0.0117 (6)	0.0019 (6)
O4	0.0700 (11)	0.1141 (16)	0.0515 (10)	−0.0003 (10)	−0.0026 (8)	−0.0018 (9)

O5	0.0552 (9)	0.0586 (9)	0.0601 (9)	0.0022 (6)	0.0121 (7)	0.0055 (6)
O6	0.0523 (9)	0.0552 (9)	0.0675 (10)	0.0009 (6)	0.0103 (7)	−0.0031 (6)
O7	0.0554 (10)	0.0697 (11)	0.0822 (12)	−0.0094 (7)	0.0150 (8)	−0.0105 (8)
O8	0.0737 (11)	0.0561 (10)	0.0786 (12)	0.0055 (7)	0.0110 (9)	0.0073 (7)
N1	0.0591 (11)	0.0613 (11)	0.0629 (12)	0.0001 (8)	0.0058 (9)	−0.0016 (8)

Geometric parameters (Å, º)

B1—O1	1.457 (3)	C4—C5	1.503 (3)
B1—O3	1.472 (3)	C4—O5	1.321 (3)
B1—O5	1.474 (3)	C4—O8	1.211 (3)
B1—O6	1.454 (3)	C5—H5A	0.9700
C1—C2	1.497 (3)	C5—H5B	0.9700
C1—O1	1.327 (3)	C5—C6	1.491 (3)
C1—O2	1.207 (3)	C6—O6	1.321 (3)
C2—H2A	0.9700	C6—O7	1.210 (3)
C2—H2B	0.9700	N1—H1A	0.875 (15)
C2—C3	1.502 (3)	N1—H1B	0.830 (15)
C3—O3	1.320 (3)	N1—H1C	0.859 (15)
C3—O4	1.207 (3)	N1—H1D	0.867 (15)
O1—B1—O3	112.42 (17)	O8—C4—O5	120.9 (2)
O1—B1—O5	108.36 (18)	C4—C5—H5A	108.3
O3—B1—O5	109.46 (18)	C4—C5—H5B	108.3
O6—B1—O1	105.67 (17)	H5A—C5—H5B	107.4
O6—B1—O3	108.43 (18)	C6—C5—C4	115.73 (19)
O6—B1—O5	112.51 (17)	C6—C5—H5A	108.3
O1—C1—C2	116.00 (18)	C6—C5—H5B	108.3
O2—C1—C2	124.1 (2)	O6—C6—C5	116.89 (19)
O2—C1—O1	119.9 (2)	O7—C6—C5	122.9 (2)
C1—C2—H2A	108.5	O7—C6—O6	120.2 (2)
C1—C2—H2B	108.5	C1—O1—B1	121.11 (17)
C1—C2—C3	114.89 (19)	C3—O3—B1	120.08 (17)
H2A—C2—H2B	107.5	C4—O5—B1	120.90 (18)
C3—C2—H2A	108.5	C6—O6—B1	121.61 (18)
C3—C2—H2B	108.5	H1A—N1—H1B	110 (2)
O3—C3—C2	116.73 (18)	H1A—N1—H1C	108 (2)
O4—C3—C2	122.6 (2)	H1A—N1—H1D	106 (2)
O4—C3—O3	120.6 (2)	H1B—N1—H1C	115 (2)
O5—C4—C5	116.80 (19)	H1B—N1—H1D	111 (2)
O8—C4—C5	122.3 (2)	H1C—N1—H1D	107 (2)
C1—C2—C3—O3	29.3 (3)	O3—B1—O1—C1	33.4 (3)
C1—C2—C3—O4	−150.8 (2)	O3—B1—O5—C4	86.0 (2)
C2—C1—O1—B1	1.7 (3)	O3—B1—O6—C6	−87.6 (2)
C2—C3—O3—B1	6.9 (3)	O4—C3—O3—B1	−172.9 (2)
C4—C5—C6—O6	−28.2 (3)	O5—B1—O1—C1	−87.7 (2)
C4—C5—C6—O7	154.0 (2)	O5—B1—O3—C3	82.4 (2)

C5—C4—O5—B1	5.0 (3)	O5—B1—O6—C6	33.6 (3)
C5—C6—O6—B1	−2.9 (3)	O5—C4—C5—C6	26.9 (3)
O1—B1—O3—C3	−38.1 (3)	O6—B1—O1—C1	151.48 (19)
O1—B1—O5—C4	−151.11 (17)	O6—B1—O3—C3	−154.56 (18)
O1—B1—O6—C6	151.66 (19)	O6—B1—O5—C4	−34.7 (3)
O1—C1—C2—C3	−33.8 (3)	O7—C6—O6—B1	175.0 (2)
O2—C1—C2—C3	145.9 (2)	O8—C4—C5—C6	−152.8 (2)
O2—C1—O1—B1	−178.0 (2)	O8—C4—O5—B1	−175.3 (2)

Hydrogen-bond geometry (Å, º)

D—H···*A*	*D*—H	H···*A*	*D*···*A*	*D*—H···*A*
N1—H1*A*···O2^{i}	0.88 (2)	2.41 (2)	3.103 (3)	137 (2)
N1—H1*A*···O4^{ii}	0.88 (2)	2.43 (2)	3.166 (3)	142 (2)
N1—H1*B*···O4^{iii}	0.83 (2)	2.32 (2)	2.970 (3)	136 (3)
N1—H1*C*···O7	0.86 (2)	2.03 (2)	2.864 (3)	165 (3)
N1—H1*D*···O8^{iv}	0.87 (2)	2.13 (2)	2.985 (3)	168 (3)
C2—H2*A*···O7^{v}	0.97	2.33	3.218 (3)	153
C2—H2*B*···O2^{vi}	0.97	2.48	3.181 (3)	129
C5—H5*B*···O6^{vii}	0.97	2.48	3.289 (3)	140

Symmetry codes: (i) −*x*+1, −*y*+2, −*z*+1; (ii) −*x*+1, *y*+1/2, −*z*+1/2; (iii) *x*+1, −*y*+3/2, *z*+1/2; (iv) *x*, *y*+1, *z*; (v) *x*−1, *y*, *z*; (vi) −*x*, −*y*+1, −*z*+1; (vii) −*x*+1, *y*−1/2, −*z*+1/2.